Ω^- and $\bar{\Omega}^+$ Production in Central Pb + Pb collisions at 40 and 158A GeV

C. Alt,[9] T. Anticic,[21] B. Baatar,[8] D. Barna,[4] J. Bartke,[6] L. Betev,[9,10] H. Białkowska,[19] A. Billmeier,[9] C. Blume,[9] B. Boimska,[19] M. Botje,[1] J. Bracinik,[3] R. Bramm,[9] R. Brun,[10] P. Bunčić,[9,10] V. Cerny,[3] P. Christakoglou,[2] O. Chvala,[15] J. G. Cramer,[17] P. Csató,[4] N. Darmenov,[18] A. Dimitrov,[18] P. Dinkelaker,[9] V. Eckardt,[14] G. Farantatos,[2] D. Flierl,[9] Z. Fodor,[4] P. Foka,[7] P. Freund,[14] V. Friese,[7] J. Gál,[4] M. Gaździcki,[9,12] G. Georgopoulos,[2] E. Gładysz,[6] K. Grebieszkow,[20] S. Hegyi,[4] C. Höhne,[13] K. Kadija,[21] A. Karev,[14] M. Kliemant,[9] S. Kniege,[9] V. I. Kolesnikov,[8] T. Kollegger,[9] E. Kornas,[6] R. Korus,[12] M. Kowalski,[6] I. Kraus,[7] M. Kreps,[3] M. van Leeuwen,[1] P. Lévai,[4] L. Litov,[18] B. Lungwitz,[9] M. Makariev,[18] A. I. Malakhov,[8] C. Markert,[7] M. Mateev,[18] B. W. Mayes,[11] G. L. Melkumov,[8] C. Meurer,[9] A. Mischke,[7] M. Mitrovski,[9] J. Molnár,[4] St. Mrówczyński,[12] G. Pálla,[4] A. D. Panagiotou,[2] D. Panayotov,[18] A. Petridis,[2] M. Pikna,[3] L. Pinsky,[11] F. Pühlhofer,[13] J. G. Reid,[17] R. Renfordt,[9] A. Richard,[9] C. Roland,[5] G. Roland,[5] M. Rybczyński,[12] A. Rybicki,[6,10] A. Sandoval,[7] H. Sann,[7,*] N. Schmitz,[14] P. Seyboth,[14] F. Siklér,[4] B. Sitar,[3] E. Skrzypczak,[20] G. Stefanek,[12] R. Stock,[9] H. Ströbele,[9] T. Susa,[21] I. Szentpétery,[4] J. Sziklai,[4] T. A. Trainor,[17] D. Varga,[4] M. Vassiliou,[2] G. I. Veres,[4,5] G. Vesztergombi,[4] D. Vranić,[7] A. Wetzler,[9] Z. Włodarczyk,[12] I. K. Yoo,[16] J. Zaranek,[9] and J. Zimányi[4]

(NA49 Collaboration)

[1]*NIKHEF, Amsterdam, The Netherlands*
[2]*Department of Physics, University of Athens, Athens, Greece*
[3]*Comenius University, Bratislava, Slovakia*
[4]*KFKI Research Institute for Particle and Nuclear Physics, Budapest, Hungary*
[5]*Massachusetts Institute of Technology, Cambridge, Massachusetts, USA*
[6]*Institute of Nuclear Physics, Cracow, Poland*
[7]*Gesellschaft für Schwerionenforschung (GSI), Darmstadt, Germany*
[8]*Joint Institute for Nuclear Research, Dubna, Russia*
[9]*Fachbereich Physik der Universität, Frankfurt, Germany*
[10]*CERN, Geneva, Switzerland*
[11]*University of Houston, Houston, Texas, USA*
[12]*Institute of Physics Świetokrzyska Academy, Kielce, Poland*
[13]*Fachbereich Physik der Universität, Marburg, Germany*
[14]*Max-Planck-Institut für Physik, Munich, Germany*
[15]*Institute of Particle and Nuclear Physics, Charles University, Prague, Czech Republic*
[16]*Department of Physics, Pusan National University, Pusan, Republic of Korea*
[17]*Nuclear Physics Laboratory, University of Washington, Seattle, Washington, USA*
[18]*Atomic Physics Department, Sofia University St. Kliment Ohridski, Sofia, Bulgaria*
[19]*Institute for Nuclear Studies, Warsaw, Poland*
[20]*Institute for Experimental Physics, University of Warsaw, Warsaw, Poland*
[21]*Rudjer Boskovic Institute, Zagreb, Croatia*

(Received 6 September 2004; published 18 May 2005)

Results are presented on Ω production in central Pb + Pb collisions at 40 and 158A GeV beam energy. For the first time in heavy ion reactions, rapidity distributions and total yields were measured for the sum $\Omega^- + \bar{\Omega}^+$ at 40A GeV and for Ω^- and $\bar{\Omega}^+$ separately at 158A GeV. The yields are strongly underpredicted by the string-hadronic URQMD model but agree better with predictions from hadron gas models.

DOI: 10.1103/PhysRevLett.94.192301 PACS numbers: 25.75.Dw

The measurement of multistrange particles is of particular interest in heavy ion collisions at ultrarelativistic energies. One important aspect is the observation that the inverse slope parameter T of the Ω m_t spectrum [1] is significantly smaller than expected from the linear mass dependence of T naively implied by the presence of radial flow. This led to the hypothesis that multistrange hyperons are not affected by the pressure generated by the hadronic matter in later stages of the reaction [2]. Originally, the increase of the production of multistrange particles as compared to elementary hadron-hadron collisions was suggested as a signature of quark-gluon plasma formation [3]. However, existing experimental data on Ξ and Λ production at lower beam energies [4,5] exhibit a much stronger enhancement than observed at top CERN SPS energies. Generally, it is found that the abundances of strange particles are close to those calculated in statistical models assuming the creation of an equilibrated hadron gas

[6]. In a hadronic environment, as expected at lower beam energies, this equilibration is generally difficult to achieve. At larger energy densities, when the hadronic system might be close to the quark-gluon plasma (QGP) phase boundary, multiparticle fusion processes could lead to fast equilibration [7]. However, there exists no dynamic explanation in a hadronic scenario at lower energy densities. The present measurement of Ω at 40A GeV provides an important test for these models. Recent results on the energy dependence of the ratio $\langle K^+\rangle/\langle\pi\rangle$ [8,9] indicate a sharp maximum of relative strangeness production at a beam energy of 30A GeV. This observation can be interpreted as a signal for the onset of deconfinement [10] and might be reflected in the energy dependence of multistrange particle production.

The data were taken with the NA49 large acceptance hadron spectrometer at the CERN SPS. With this detector, tracking is performed by four large-volume time projection chambers (TPCs). A measurement of the specific energy loss dE/dx provides particle identification at forward rapidities. Time-of-flight detectors improve the particle identification at midrapidity. Centrality selection is based on a measurement of the energy deposited in a forward calorimeter by the projectile spectators. A detailed description of the apparatus can be found in [11].

We present in this Letter an analysis of two samples of central Pb + Pb events taken at beam energies of 40 and 158A GeV in the years 1999 and 2000, respectively. About 5.8×10^5 events were recorded at 40A GeV with a centrality selection of 7.2% of the total inelastic cross section corresponding, on average, to $\langle N_w\rangle = 349$ wounded nucleons [12]. At 158A GeV, 2.8×10^6 events were taken at 23.5% centrality corresponding to $\langle N_w\rangle = 262$.

The Ω were identified in the decay channel $\Omega \rightarrow \Lambda K$, $\Lambda \rightarrow p\pi$ (68% branching fraction). To reconstruct the $\Omega^-(\bar{\Omega}^+)$, the $\Lambda(\bar{\Lambda})$ candidates were selected in an invariant-mass window of 1.101–1.131 GeV/c^2 and combined with all negatively (positively) charged tracks in the event. The same procedure as in the Ξ analysis of [13] was used to identify the secondary vertex of the Ω decay.

To reduce the combinatorial background several cuts were applied. Identification of the (anti-)protons by dE/dx in the TPCs reduced the contribution from fake $\Lambda(\bar{\Lambda})$. The measured dE/dx was required to be within 3.5 standard deviations from the predicted Bethe-Bloch value. Likewise an enriched kaon sample was extracted from the charged tracks. A further background reduction was achieved by requiring a minimal distance of 25 cm in the beam direction between the target and the Ω decay vertex position. The Ω candidates were extrapolated back to the target plane to obtain the transverse coordinates b_x (magnetic bending plane) and b_y of the impact point with respect to the primary interaction vertex. To reject non-vertex candidates, cuts of $|b_x| < 0.5$ cm and $|b_y| < 0.25$ cm were applied. Kaons from the primary vertex were excluded by imposing a cut of $|b_y| > 1.0$ cm on the kaon tracks. In addition, $|b_y| > 0.4$ cm was required for the Λ candidates at 40A GeV. With these cuts an acceptable separation of signal and background was achieved for Ω transverse momenta above 0.9 GeV/c.

In Fig. 1 the invariant-mass distributions of the Ω^- and $\bar{\Omega}^+$ candidates are shown for $p_t > 0.9$ GeV/c and $-0.5 < y < 0.5$. Note that the available statistics at 40A GeV is not sufficient to separately analyze the Ω^- and $\bar{\Omega}^+$ [14]. Clear signals are observed at the Ω mass of $m_0 = 1672.5$ MeV/c^2 [15] with a resolution of 5 and 4 MeV/c^2 at 40 and 158A GeV, respectively.

The spectra were fitted to the sum of a polynomial background and a signal distribution, determined from the simulation described below. The raw Ω yield is obtained by subtracting the fitted background in a mass window of ± 7 MeV/c^2 around the nominal Ω mass.

Detailed simulations were made to correct the yields for geometrical acceptance and losses in the reconstruction. For this purpose, a sample of Ω was generated in the full phase space accessible to the experiment. The GEANT 3.21 package [16] was used to track the generated Ω and their decay particles through a detailed description of the NA49 detector geometry. NA49 specific software was used to simulate the TPC response taking into account all known detector effects. The simulated signals were added to those of real events and subjected to the same reconstruction procedure as the experimental data. The acceptance and efficiency were calculated in bins of p_t and y as the fraction of the generated Ω which traverse the detector, survive the reconstruction and pass the analysis cuts. This fraction amounts in total to 0.4–0.5% (0.2–0.5%) for 40(158)A GeV data, depending on p_t and y. The geometric acceptance is of the order of 20%, which

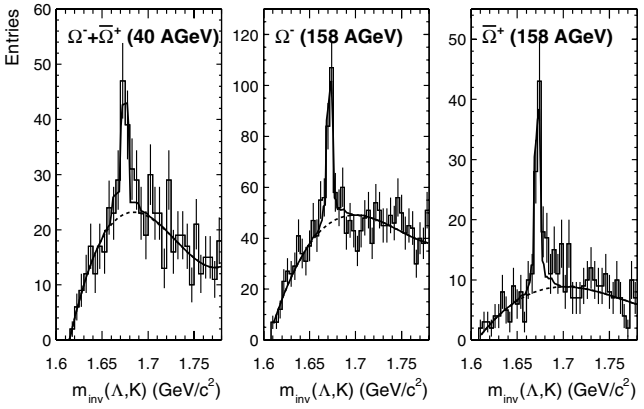

FIG. 1. The invariant-mass distributions of Ω^- and $\bar{\Omega}^+$ candidates. Left: summed distribution of ΛK^- and $\bar{\Lambda} K^+$ pairs at 40A GeV. Middle: ΛK^- pairs at 158A GeV. Right: $\bar{\Lambda} K^+$ pairs at 158A GeV. The solid curves represent a fit to signal and background described in the text. The dashed curves show the background contribution.

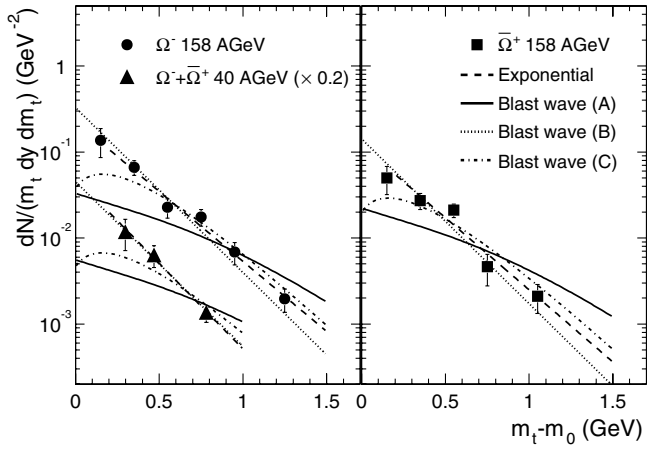

FIG. 2. The transverse-mass spectra of Ω^- and $\bar{\Omega}^+$ at midrapidity. Left: $\Omega^- + \bar{\Omega}^+$ at 40A GeV (triangles) and Ω^- at 158A GeV (circles). Right: $\bar{\Omega}^+$ at 158A GeV. The errors shown are statistical only. The dashed curve shows the exponential fit described in the text. The solid, dotted, and dash-dotted curves show a model including transverse expansion.

in turn is reduced to 0.6–1.2% by the cuts that suppress the combinatorial background. A further reduction of the reconstruction efficiency at 158A GeV by 30–60% is due to the high track density.

The statistical error is given by the quadratic sum of three contributions: the signal, the background and the efficiency correction, the latter being smaller at 40 than at 158A GeV. The systematic uncertainties are dominated by the background subtraction method and by imperfections in the simulation. By varying the analysis strategy and the cuts applied, a systematic error of 10% is estimated in the transverse-mass region $(m_t - m_0) > 0.3$ GeV. At lower m_t this error is about 25%

In Fig. 2 the transverse-mass spectra of the Ω are shown integrated over the range ± 0.5 (40A GeV) and ± 1 (158A GeV) around midrapidity. The transverse-mass spectra were fitted to an exponential function

$$\frac{\mathrm{d}N}{m_\mathrm{t}\mathrm{d}m_\mathrm{t}\mathrm{d}y} \propto \exp\left(-\frac{m_\mathrm{t}}{T}\right) \qquad (1)$$

in the range $(m_t - m_0) > 0.2$ GeV. The results are plotted in Fig. 2 (dashed curves) and the inverse slope parameters T are listed in Table I. No significant difference can be observed in the shape of the Ω^- and $\bar{\Omega}^+$ spectra at 158A GeV. The inverse slope parameters are close to the values obtained by the WA97 and NA57 collaborations [1,17]. The inverse slope parameter at 40A GeV is somewhat lower but, within errors, compatible with the 158A GeV result.

To investigate whether the Ω decouples earlier from the fireball than lighter hadrons, we use a hydrodynamical model which assumes a transversely expanding emission source [18]. The parameters of this model are the freezeout temperature T_f and the transverse flow velocity β_s at the surface. Assuming a linear radial velocity profile $\beta_\mathrm{t}(r) = \beta_\mathrm{s} r/R$, which is motivated by hydrodynamical calculations, the m_t spectrum can be computed from

$$\frac{dN}{m_\mathrm{t}dm_\mathrm{t}dy} \propto \int_0^R r dr m_\mathrm{t} I_0\left(\frac{p_\mathrm{t}\sinh\rho}{T_\mathrm{f}}\right) K_1\left(\frac{m_\mathrm{t}\cosh\rho}{T_\mathrm{f}}\right), \qquad (2)$$

where R is the radius of the source and $\rho = \tanh^{-1}\beta_\mathrm{t}$ is the boost angle. The full curve (A) in Fig. 2 shows the result of a calculation with $T_\mathrm{f} = 90$ MeV and an average flow velocity $\langle\beta_\mathrm{t}\rangle = 0.5$. These parameters were obtained from a simultaneous fit of the model to the m_t spectra of K^+, K^-, p, $\bar{p}$, ϕ, Λ, and $\bar{\Lambda}$, all measured by NA49 at 158A GeV [4,8,19,20]. The dotted curve (B) is calculated with $T_\mathrm{f} = 170$ MeV and $\langle\beta_\mathrm{t}\rangle = 0.2$, obtained from a fit to J/ψ and ψ' spectra [21]. The disagreement of curve (A) and the agreement of curve (B) with the data suggest that in this version of the model, the freezeout conditions of the Ω are similar to those of the J/ψ or ψ' but are different from those of the lighter hadrons. The use of a constant expansion velocity, on the other hand, results in a fair agreement of the measured hadron spectra, including the Ξ and the Ω, with $T_\mathrm{f} = 127$ MeV and $\langle\beta_\mathrm{t}\rangle = 0.5$ [22], as shown by curve (C) for the Omega. It predicts, however, a significant decrease of the spectrum for heavy hadrons for $m_t - m_0 \rightarrow 0$. This dip is already quite pronounced for the Omega but not suggested by the measurements [23]. Thus, a radius independent transverse expansion velocity may be too crude an approximation of the velocity profile.

The parameterizations of Eqs. (1) and (2) were used to extrapolate the Ω yields into the unmeasured regions of m_t. Assuming that the shape of the m_t distribution does not depend on rapidity, extrapolation factors of 2.3 (2.2) at

TABLE I. The inverse slope parameter T (MeV), the width σ of the rapidity distribution, the midrapidity yield dN/dy and the total yield $\langle N\rangle$ of Ω production at 40 and 158A GeV. The first error is statistical and the second systematic.

	40A GeV $\Omega^- + \bar{\Omega}^+$	158A GeV Ω^-	158A GeV $\bar{\Omega}^+$
T	$218 \pm 39 \pm 39$	$267 \pm 26 \pm 10$	$259 \pm 35 \pm 18$
σ	$0.6 \pm 0.1 \pm 0.1$	$1.2 \pm 0.4 \pm 0.2$	$1.0 \pm 0.4 \pm 0.2$
$\mathrm{d}N/\mathrm{d}y$	$0.10 \pm 0.02 \pm 0.02$	$0.14 \pm 0.03 \pm 0.01$	$0.07 \pm 0.02 \pm 0.01$
$\langle N\rangle$	$0.14 \pm 0.03 \pm 0.04$	$0.43 \pm 0.09 \pm 0.03$	$0.19 \pm 0.04 \pm 0.02$

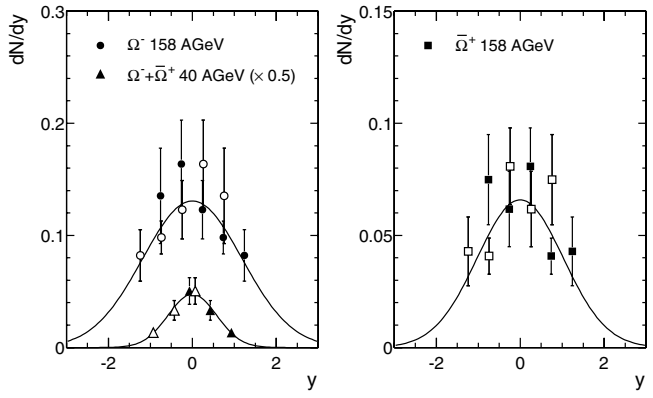

FIG. 3. The rapidity dependence of Ω production in central Pb + Pb collisions. Left: $\Omega^- + \bar{\Omega}^+$ at 40A GeV (triangles) and Ω^- at 158A GeV (circles). Right: $\bar{\Omega}^+$ at 158A GeV. The errors shown are statistical only. The open symbols show the measured points (full symbols) reflected around midrapidity. The curves correspond to Gaussian fits to the data.

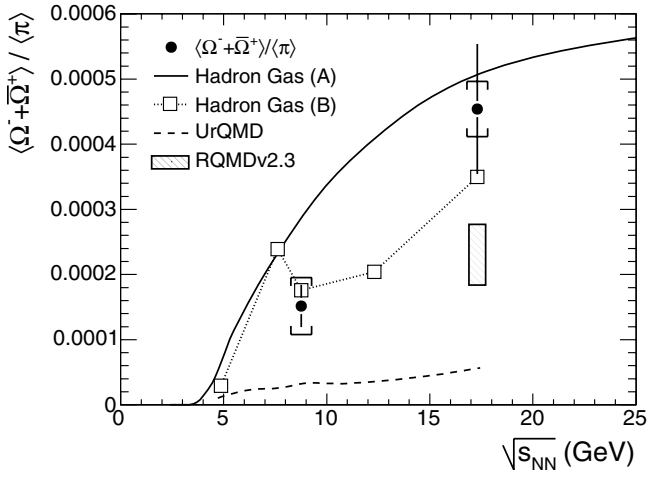

FIG. 4. The ratio $\langle\Omega\rangle/\langle\pi\rangle$ (see text) versus the center-of-mass energy. Statistical errors are shown as lines, while the brackets denote the systematic errors. The dashed curve shows the prediction from the hadronic string model URQMD [25] and the gray box that of RQMD [26]. A hadron gas model without strangeness suppression [28] is shown by the solid curve. The open squares represent the fits from [27] including strangeness undersaturation.

40(158)A GeV were obtained from fits to the summed Ω^- and $\bar{\Omega}^+$ data. A systematic uncertainty of 6% is due to the choice of parameterization.

The extrapolated Ω yields at 40 and 158A GeV are shown in Fig. 3 as a function of rapidity. All spectra can be described by a Gaussian with zero mean and a width σ obtained from a fit to the data; see Table I. The widths of the Ω^- and $\bar{\Omega}^+$ spectra at 158A GeV are compatible but are both significantly larger than the width measured at 40A GeV. Also given in Table I are the midrapidity yields dN/dy ($-0.5 < y < 0.5$) and the total yields $\langle N\rangle$ obtained by extrapolating the rapidity spectra into the unmeasured region using the Gaussian fits. The midrapidity yields are slightly below the values given by the NA57 collaboration [24]; however, they agree within statistical errors, if the difference in the centrality selection at 158A GeV is taken into account.

In the following we denote by $\langle\Omega\rangle$ the sum of the total Ω^- and $\bar{\Omega}^+$ yields and by $\langle\pi\rangle$ the total charged pion yields from [8], multiplied by a factor of 1.5. The pion yields at 158A GeV were scaled by the ratio of the numbers of wounded nucleons to account for the difference in the centrality selection of the pion and the Ω measurement (note the centrality selection at 40A GeV of 7% and at 158A GeV of 23.5% most central events). Figure 4 shows the ratio $\langle\Omega\rangle/\langle\pi\rangle$ as function of the center-of-mass energy. The ratio tends to increase with energy. It is clearly underpredicted by the URQMD string-hadronic model [25] as shown by the dashed curve in Fig. 4. A better description of the 158A GeV data is provided by RQMD version 2.3 including the color rope mechanism [26].

On the other hand, the data are close to the predictions of statistical hadron gas models which use a grand canonical ensemble. In these models, the chemical freezeout temperature and the baryonic chemical potential are fitted to the yields of other measured hadrons. The hadron gas model of [27] (labeled B in Fig. 4) introduces in addition a strangeness undersaturation parameter γ_s in the fits, which have been performed at each energy separately. The fit results at 30A GeV reflect the sharp maximum of the K^+/π^+ ratio observed around this energy. The present measurement at 40A GeV seems to favor this model, compared to that of [28] (labeled A in Fig. 4) which does not allow for strangeness undersaturation ($\gamma_s = 1$ for all energies). The data point at 158A GeV, however, does not discriminate between the two models. Nevertheless, the observation that Ω production is compatible with phase-space undersaturation at higher SPS energies (> 30AGeV), would be in line with a similar behavior of the kaon excitation function in the same energy regime [9].

In summary, NA49 has performed a measurement of Ω production in central Pb + Pb reactions over a wide region of phase space. At a beam energy of 158A GeV the available statistics allowed us to separately analyze Ω^- and $\bar{\Omega}^+$. The shapes of the transverse-mass spectra at this energy reveal no difference between Ω^- and $\bar{\Omega}^+$ and are in agreement with previous results by WA97 and NA57. In a hydrodynamically inspired model with radially increasing velocity profile, the data favor a low transverse expansion velocity and high freezeout temperature. The rapidity spectra of the Ω, which have not been measured before in heavy ion reactions, are compatible with a Gaussian shape. The widths for Ω^- and $\bar{\Omega}^+$ appear to be similar. The yields are strongly underpredicted by the string-hadronic URQMD

model. The data agree better with predictions from hadron gas models.

This work was supported by the US Department of Energy Grant No. DE-FG03-97ER41020/A000; the Bundesministerium für Bildung und Forschung and the Virtual Institute VI-146 of the Helmholtz Gemeinschaft, Germany; the Polish State Committee for Scientific Research (2 P03B 130 23, SPB/CERN/P-03/Dz 446/ 2002-2004, 2 P03B 04123); the Hungarian Scientific Research Fund, OTKA (T032648, T032293, T043514, F034707); the Polish-German Foundation; and the Korea Research Foundation Grant (KRF-2003-070-C00015).

*Deceased.

[1] F. Antinori *et al.* (WA97 Collaboration), Eur. Phys. J. C **14**, 633 (2000).
[2] H. van Hecke, H. Sorge, and N. Xu, Phys. Rev. Lett. **81**, 5764 (1998).
[3] J. Rafelski and B. Müller, Phys. Rev. Lett. **48**, 1066 (1982).
[4] T. Anticic *et al.* (NA49 Collaboration), Phys. Rev. Lett. **93**, 022302 (2004).
[5] P. Chung *et al.* (E895 Collaboration), Phys. Rev. Lett. **91**, 202301 (2003).
[6] F. Becattini, J. Cleymans, A. Keranen, E. Suhonen, and K. Redlich, Phys. Rev. C **64**, 024901 (2001).
[7] P. Braun-Munzinger, J. Stachel, and C. Wetterich, Phys. Lett. B **596**, 61 (2004).
[8] S. V. Afanasiev *et al.* (NA49 Collaboration), Phys. Rev. C **66**, 054902 (2002).
[9] M. Gaździcki *et al.* (NA49 Collaboration), J. Phys. G **30**, S701 (2004).
[10] M. Gaździcki and M. I. Gorenstein, Acta Phys. Pol. B **30**, 2705 (1999).
[11] S. V. Afanasiev *et al.* (NA49 Collaboration), Nucl. Instrum. Methods Phys. Res., Sect. A **430**, 210 (1999).
[12] A. Białas, M. Błeszyński, and W. Czyż, Nucl. Phys. **B111**, 461 (1976).
[13] S. V. Afanasiev *et al.* (NA49 Collaboration), Phys. Lett. B **538**, 275 (2002).
[14] M. Mitrovski, Diploma Thesis, University of Frankfurt, 2004.
[15] K. Hagiwara *et al.* (Particle Data Group), Phys. Rev. D **66**, 010001 (2002).
[16] R. Brun *et al.*, GEANT 3 manual, CERN Program Library Long Writeup W5013, 1994.
[17] F. Antinori *et al.*, J. Phys. G **30**, 823 (2004).
[18] E. Schnedermann and U. Heinz, Phys. Rev. C **50**, 1675 (1994).
[19] T. Anticic *et al.* (NA49 Collaboration), Phys. Rev. C **69**, 024902 (2004).
[20] S. V. Afanasiev *et al.* (NA49 Collaboration), Phys. Lett. B **491**, 59 (2000).
[21] M. I. Gorenstein, K. A Bugaev, and M. Gaździcki, Phys. Rev. Lett. **88**, 132301 (2002).
[22] M. van Leeuwen *et al.* (NA49 Collaboration), Nucl. Phys. **A715**, 161c (2003).
[23] Note that the transverse-mass spectra at 158*A* GeV presented here deviate in the first data point from the result of a preliminary analysis shown in [22].
[24] F. Antinori *et al.*, Phys. Lett. B **595**, 68 (2004).
[25] M. Bleicher *et al.*, J. Phys. G **25**, 1859 (1999); private communication.
[26] U. Heinz, J. Sollfrank, H. Sorge, and N. Xu, Phys. Rev. C **59**, 1637 (1999).
[27] F. Becattini, M. Gaździcki, A. Keränen, J. Manninen, and R. Stock, Phys. Rev. C **69**, 024905 (2004).
[28] P. Braun-Munzinger, J. Cleymans, H. Oeschler, and K. Redlich, Nucl. Phys. A **697**, 902 (2002); private communication.